Ultrasonics Sonochemistry 84 (2022) 105978

Contents lists available at ScienceDirect

Ultrasonics Sonochemistry

journal homepage: www.elsevier.com/locate/ultson

Dual-frequency power ultrasound effects on the complexing index, physicochemical properties, and digestion mechanism of arrowhead starch-lipid complexes

Husnain Raza [a,c,1], Qiufang Liang [a,1], Kashif Ameer [d], Haile Ma [a,b], Xiaofeng Ren [a,b,*]

[a] Jiangsu University, School of Food and Biological Engineering, Zhenjiang, Jiangsu 212013, China
[b] Institute of Food Physical Processing, Jiangsu University, 301 Xuefu Road, Zhenjiang, Jiangsu 212013, China
[c] Institute for Advanced Study (IAS), Shenzhen University, No. 3688, Nanhai Avenue, Nanshan District, Shenzhen, Guangdong 518060, China
[d] Institute of Food Science and Nutrition, University of Sargodha, Sargodha 40100, Pakistan

ARTICLE INFO

Keywords:
Arrowhead
Resistant starch
Physicochemical
Characterization
Digestion
Ultrasound
Fatty acid
Starch-lipid complex

ABSTRACT

Multi-scale structural interactions of the arrowhead starch-linoleic/stearic acid complexes under different durations (20, 40 & 60 min) of dual-frequency power ultrasound (DFPU, 20/40 kHz) and their underlying mechanisms were discussed. Differential scanning calorimetry and X-ray diffraction (XRD) revealed V6 type (V6-I, II) crystalline structure for ultrasonically-treated arrowhead starch-linoleic acid (UTAS-LA) complexes. An increased degree of short-range molecular order as IR ratios of 1045/1022 cm^{-1} was evident from the FTIR results. The complexing index (CI) values of the complexes were greater than 65%, and the highest CI values of 83.04% and 81.26% were found in the case of UTAS-LA40 and UTAS-LA60, respectively. SEM results showed that LA-complexes had a sponge-like structure with smooth surfaces, while the SA-complexes exhibited flaky structures with irregular shapes and rough surfaces. The V-type complexes exhibited a higher digestion resistance than native AS and un-sonicated AS-LA/SA complexes due to partial RDS convention to RS.

1. Introduction

Arrowhead (*Sagittaria sagittifolia* L.) is one of the species of the genus *Sagittaria* belonging to the aquatic family *Alismataceae*. Since, Tang Dynasty, in Traditional Chinese Medicinal (TCM) philosophy, arrowhead tuber has been employed as the restorative, also known as Kue [1], Jiandaocao [2], Duck Potato, or Swan Potato [3]. Adequate processing is needed regarding raw tuber for removal of bitter and unpleasant taste prior to consumption by intended consumers. Looking at the nutritional profile of arrowhead, it is mainly rich in carbohydrates (54.60 g/100 g), protein (16.4 g/100 g) [6], and fat (0.47 g/100 g), including others [4,5].

The digestion of starch is an important topic to research as starches are employed to get half of the energy from foods by the human body after ingestion [7]. Based on *in-vitro* digestibility determined by the Englyst method [8], starch is divided into three fractions, namely slowly digestible starch (RDS), rapidly digestible starch (SDS), and resistant starch (RS). RDS has a high glycemic response and is digested in the small intestine. In contrast, SDS, with the comparably lower glycemic response, is digested slowly. On the other hand, RS is fermented into short-chain fatty acids by microbial action in the large intestine. The digestion of RS is not possible to render release of glucose, therefore, the RS consumption might not be useful in mitigation of the metabolic disorders and prevention of several lifestyle disorders, such as cardiovascular diseases, Type II diabetes, and obesity. Both SDS and RS are reported to cause the glycemic index lowering effect. Starchy foods having a lower degree of RDS content and high SDS and RS content can deliver many human health benefits [9,10]. From previous research, RS has been categorized into five groups (RS1 to RS5) with very different nutritional properties (most of the studies focused on RS2 and RS4) [11,12]. RS5 is recently developed and formed by complexing the amylose with lipids known as the amylose–lipid complex. The formation of V-type starch-lipid complexes usually involves the guest molecules (lipids, emulsifiers, or other aromatic compounds) embedded in the helical interior of starch and stabilized through hydrophobic interactions and hydrogen bonding.

* Corresponding author at: School of Food and Biological Engineering, Jiangsu University, 301 Xuefu Road Zhenjiang 212013, China.
E-mail address: renxiaofeng@ujs.edu.cn (X. Ren).
[1] These authors contributed equally to this work.

https://doi.org/10.1016/j.ultsonch.2022.105978
Received 22 January 2022; Received in revised form 25 February 2022; Accepted 5 March 2022
Available online 7 March 2022

Recently, the introduction of ultrasonic-assisted extraction (UAE) has brought up many advantages. Besides being an eco-friendly method, it reduces the extraction time, energy, and solvent while increasing the reaction rate and extraction yield [13–15]. Also, the extraction through sonication is responsible for changing the structure, molecular weight, and glycosidic linkages based on the origin of the starch, physical state, the concentration of slurry, and conditions used for the sonication process, including time, temperature, frequency, and power [16–18]. Furthermore, the use of ultrasonication is accepted as an emerging concept of "green chemistry and technology" to process food for eco-friendly applications [14]. According to Wang et al. [19], the ultrasound can change the starch's physicochemical properties, ultimately changing the supramolecular structure and making the starch susceptible to enzymatic hydrolysis depending on the treatment conditions of ultrasound. Wang et al. [20] has recently studied the effect of different treatment methods to understand the properties of the potato starch-lauric acid complex. Upon the use of ultrasound at a power density of 320 W/cm^2 for 10 min interval, an increase in the release of amylose molecules was observed as facilitated by the ultrasonic treatment. In another study by [21], the corn starch-lipid complex was formed using ultrasonication for 15 min at 320 W/cm^2 and an interval pulse of 4 s. The lipids included were octanoic acid (OA), capric acid (CA), and lauric acid (LA) in a liquid and solid state. The properties of the complexes were significantly affected by the physical state of the lipids and applied ultrasonication conditions. Microwave and ultrasonication food processing were also used by Zhao and his team [22] to understand the physicochemical properties of lotus starch complexed with green tea polyphenols. While understanding the digestibility mechanism of ultrasonically regulated retrograded corn starch, [7] discovered that ultrasonication was also useful to facilitate the complexation of amylose with lipid as arbitrated by the XRD and DSC exothermic peaks results with V-type complex.

The authors also found that ultrasonication could be used as a potential approach to control the digestion of starch-rich foods. Furthermore, comparative studies have proved that dual-frequency ultrasound is more effective for processing modified starches, which can be used in food or other chemical industries [23]. However, the reports on the elucidation of mechanistic details of starch-lipid complexes under the physical field are still lacking with a profound understanding of the digestibility of starch-lipid compounds. Therefore, this study was aimed to select dual-frequency (20/40 kHz) ultrasound for different treatment times of 20, 40, and 60 min and the fatty acid in liquid (linoleic acid) and solid (stearic acid) state to complex with native arrowhead starch to systematically understand the effects of ultrasonic treatment on the multi-scale structure of the composites and influence of these interactions on digestibility. The structure and morphology of these complexes were characterized by X-ray diffraction (XRD), differential scanning calorimetry (DSC), Fourier transforms infrared spectroscopy (FTIR), and scanning electron microscope (SEM). This is the first study to characterize arrowhead resistant starch (RS5) using dual-frequency ultrasonication to the best of our knowledge. Our work will further give insights into ultrasound as green processing on the interaction of starch and lipids in different states, which will help in controlling the quality of foods and help in formulating a more sophisticated food for patients with type 2 diabetes.

2. Materials and methods

Procurement of the arrowhead tubers was carried out from the local market named "JiangDa Farmer's Market" located in the vicinity of Jiangsu University, Zhenjiang, China. The extraction of arrowhead starch was performed as per the following procedure of Qin et al. [24]. Linoleic acid (LA) and stearic acid (SA) as well as amyloglucosidase (AMG) (No. 9913, 2500 U/mg) and porcine pancreatic α-amylase (PPA) (10 U/mg) were procured from Sigma–Aldrich Chemical Co. (St. Louis, MO, USA).

2.1. Preparation of starch-lipid complex under ultrasound

RS5 was prepared by using the method of [21]. LA and SA (10%, dry starch basis) were stirred with starch at 90 °C for 20 min. The pastes were then sealed into high-pressure resistant plastic bags and sonicated at 20/40 kHz for 20, 40, and 60 min with on and off intervals of 10 s and 4 s, respectively at 300 W/L power density by means of ultrasonic bath (manufactured at Jiangsu University with 20,084,798 Model no.) as depicted in Fig. 1. The samples were named as ultrasonically-treated arrowhead starch-linoleic/stearic acid complex UTAS-LAx/SAx, where × represented the time of sonication as 20, 40, and 60 min. A coldwater bath equipped with the thermostat was used to set the temperature at 20 °C. The sonicated samples were centrifuged at 4000 rpm for 10 min and washed three times with a 50% ethanol/water mixture to remove the uncomplexed or free fatty acids. The pastes not exposed to ultrasound treatment (UT) were also centrifuged and washed. Finally, the precipitates were dried at 40 °C for 24 h and kept in a desiccator for further use.

2.2. Complexing index (CI) value determination

The inclusion complex formation of arrowhead starch-linoleic acid (AS-LA/SA) was determined by the CI value [16]. Two grams of dried samples were weighed and mixed with the distilled water (20 mL) followed by heating at 95 °C for 30 min with continuous mixing. After heating, 5 g of pastes were taken and transferred to centrifuge tubes of 50 mL followed by distilled water addition in an amount of 25 mL. The vortexing of centrifuge tubes was carried out for 2 min and then subjected to centrifugation at 4000 rpm for 15 min intervals. Aliquots in an amount of 500 uL were taken and thoroughly mixed with the distilled water (15 mL) and 2 mL of iodine solution (2.0 g of KI, 1.3 g of I_2, and distilled water of 100 mL). The supernatant was analyzed for absorbance using a UV–Vis spectrophotometer (Varian Inc., Palo Alto, USA) at 690 nm (A_s). The starch paste (without LA/SA) was subjected to spectrophotometric analysis by employing as the reference (A_o). The following equation was used to determine the values of CI.

$$CI(\%) = \frac{(Ao - As)}{Ao} \times 100 \quad (1)$$

2.3. FTIR analysis of starch-lipid complex

The functional groups' analysis of AS-LA/SA complexes was carried out by means of Fourier Transform Infrared Spectroscopy (FTIR) through Tensor-27 FTIR spectrometer (Nicolet IS50, Thermo Electron Corp., USA). Samples (2 mg) were milled with that of the KBr pellets (100 mg) and FTIR spectra were observed from in the spectral range of 4000 to 400 cm^{-1} by scan accumulation rate of 32 scans at 4 cm^{-1} resolution.

2.4. X-ray diffraction patterns of starch-lipid complex

The changes in crystallinity of the AS-LA complexes were elucidated through the diffractometer (D8 Advance, Bruker AXS Advanced X-ray Solutions GmbH, Karlsruhe, Germany). The XRD diffractograms were analyzed with the generator voltage and current set at 45 kV and 40 mA, respectively in conjunction with the samples scanning at 2θ angle ranging from 4° to 40° in 0.02° steps at 1 s/step.

2.5. Thermal properties (DSC)

AS-LA/SA complexes (3–5 mg dB) were taken in the stainless steel pans and weighed and about 16 uL of distilled water was mixed with by means of a microsyringe. Then, the pans were subjected to hermetical sealing. Moreover, the equilibration of the samples was also carried out at ambient room temperature for 24 h time intervals prior to scanning.

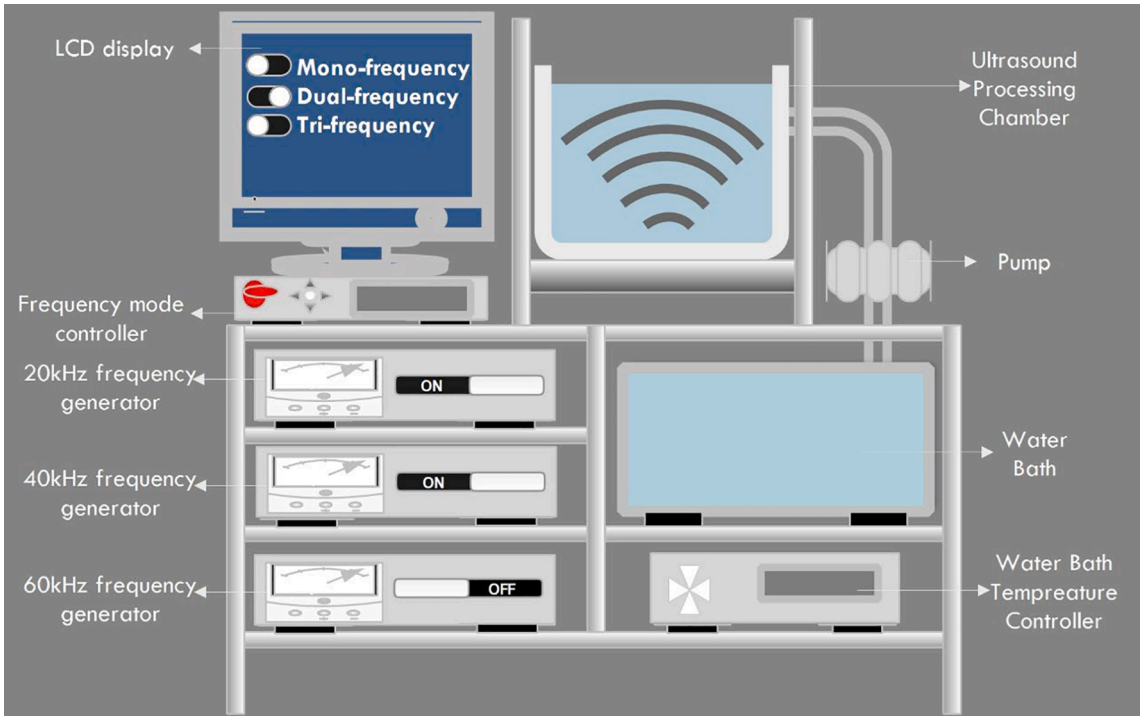

Fig. 1. Pictorial scheme of multi-frequency power ultrasound (MFPU) with various modes of operation: single-frequency power ultrasound (SFPU, 20, 40, 60 kHz), dual-frequency power ultrasound (DFPU, 20/40, 40/60, 20/60 kHz), and tri-frequency power ultrasound (TFPU, 20/40/60 kHz).

DSC thermograms were achieved by scanning the samples at a temperature ranging from 25 to 150 °C at a 10 °C/min rate. The determination of the DSC thermal parameters was carried out including the onset (T_o), peak (T_p), and conclusion melting temperature (T_c), as well as the enthalpy (ΔH) of the endotherms of complexes, were determined. The thermodynamic data were subjected to analysis through the DSC software (TA Instruments, New Castle, DE, USA).

2.6. Scanning electron microscopy (SEM)

Arrowhead starch powder and its respective lipid complexes (AS-LA/SA) were subjected to affixation on aluminum pin-type stubs through the use of the carbon paste. High-pressure air was employed for the removal of the excessive powder. Samples coating was also performed with the aid of the gold–palladium by means of the mini sputter. The samples were photographed to elucidate the microstructural changes through the use of a scanning electron microscope (SEM) (Hitachi S-3400 N, Hitachi High Tech., Tokyo, Japan) at 500–5000 × resolution.

2.7. Particle size distribution (PSD) analysis

The AS and AS/LA/SA complexes were analyzed for their respective particle size distributions by employing the Laser Particle Size Meter (MS 3000, Malvern Inst., Co., Ltd.). The specified amount of each dried AS and AS-LA/SA complex powder (250 mg) was mixed with the distilled water (50 mL), and the measurement of the particle size was performed at a constant refractive index of 1.33.

2.8. Ultrasonication effect on color properties of starch-lipid complex

AS and AS/LA/SA complexes were analyzed for their color properties by employing the Hunter Lab colorimeter (Model 45/0 L: Hunter Associates Lab., Indiana, USA). The color parameters of *L*, a*,* and *b** were indicative of the degrees of the lightness, redness/greenness, and yellowness/blueness, respectively, and the Hunter colorimeter was subjected to calibration for *L*, a*,* and *b** values against a white tile prior to conducting colorimetric analysis.

2.9. In vitro starch-lipid complex digestion

In vitro digestibility of arrowhead starch (AS), AS-LA/SA, and UTAS-LA/SA complexes were determined as per the reported method of Englyst with slight modifications [7]. Following digestion intervals were followed for each starch fraction as; RDS, < 20 min; SDS, 20–120 min, and RS, >120 min [25].

2.10. Statistical analyses

All the measurements were performed in triplicate (n = 3), and results were recorded as mean ± standard deviation (SD). The experimental data obtained were employed to carry out the statistical analysis of the AS complexes through one-way analysis of variance (ANOVA) and the differences between the means were compared for their statistical significance by means of Tukey's test ($p < 0.05$) using the SPSS Statistics 19.0 (IBM, Inc., New York, NY).

3. Results & discussion

3.1. CI values of the starch-lipid complexes

The values of CI of starch-lipid complexes using linoleic and stearic acid under different conditions of ultrasound are determined and results are depicted in Fig. 2. The CI values of the AS complexes with LA and SA were greater than 68%, and the highest CI values of 83.04% and 78.51% were found in the case of UTAS-LA40 and UTAS-SA40, respectively. This implied that LA exhibited a greater ability to cause the formation of complex molecules of starch when LA was subjected to specific experimental conditions. The higher CI values give the indication of the enhanced degree of formation of V-type inclusion complexes between fatty acids and amylose molecules. CI is based on starch-iodine complex formation in starch that represents the degree of starch complexed to lipids [26]. The degree of complexation was increased by increasing the

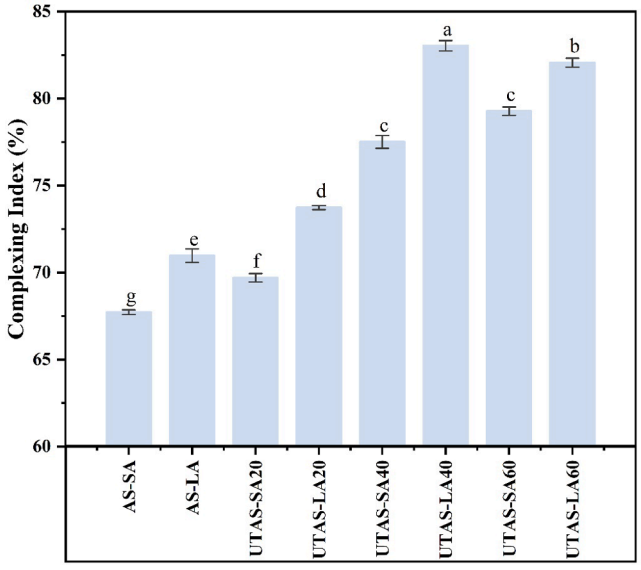

Fig. 2. Effect of DFPU on the complexing index of AS-LA/SA complexes at different sonication times.

time for sonication, and it was more profound for UTAS-LA at 40 min. The value of CI was higher for all samples of LA that showed better complexation ability of arrowhead starch with fatty acids in liquid form, probably due to the better dispersibility of liquid lipids compared to solid lipids in arrowhead starch suspension. The results were further confirmed by SEM, where AS-LA and UTAS-LA were found to have more compact and uniform distributions. The results of XRD were also consistent with CI values where the complexes of linoleic acid had increased V-type crystallinity compared with stearic acid. The values of CI rose from 68.06% to 75.98% and 70.97 to 83.04% for SA and LA, respectively. Conversely, among sonicated samples, UTAS-SA20 and UTAS-LA20 exhibited the lowest CI values of 70.20 and 74.39%, respectively. The increase in the CI values occurred due to the cavitation effect of UT, which disintegrated the swollen starch granules to release more amylose from their inner matrices resulting in enhanced availability of amylose to bind with the lipids. Moreover, higher CI values in the case of UTAS samples implied that exposure to sonication treatment might cause swollen starch granules to disintegrate accompanied by the increased mass transfer of amylose from the inner matrices of starch granules structures. The sonication process has also been reported to improve ligand dispersibility in the suspension of gelatinized starches which ultimately increased starch contact with fatty acids resulting in better v-type inclusion complex formation [21].

3.2. Changes in the crystalline structure

The X-ray diffractograms and relative crystallinities (RC) of AS and its respective complexes with LA and SA under different sonication conditions are shown in Fig. 3(a-b). All complexes were found to have prominent peaks (2θ) at 13.0° and 20.0° indicating the formation of a V-type complex [27,28]. The complexes further showed additional peaks at 2θ = 7.0° for LA and 7.5°, 9.0°, 22.0°, and 24.0° for SA. The additional peaks by SA-complexes at 22.0° and 24.0° appeared as a result of free fatty acid aggregations [26]. The free fatty acid crystals trapped around the helices of the complex could be further seen from the results of SEM micrographs (Fig. 6). On the other hand, arrowhead starch (AS) was ascribed to a typical A-type structure with peaks at 11.5°, 15.0°, 17.0°, and 23.0° (2θ).

As evident from Fig. 3 (a, b), the intensities of the peak regarding linoleic acid complex were stronger than the complexes with stearic acid, which showed a better semi-crystalline structure by liquid lipid

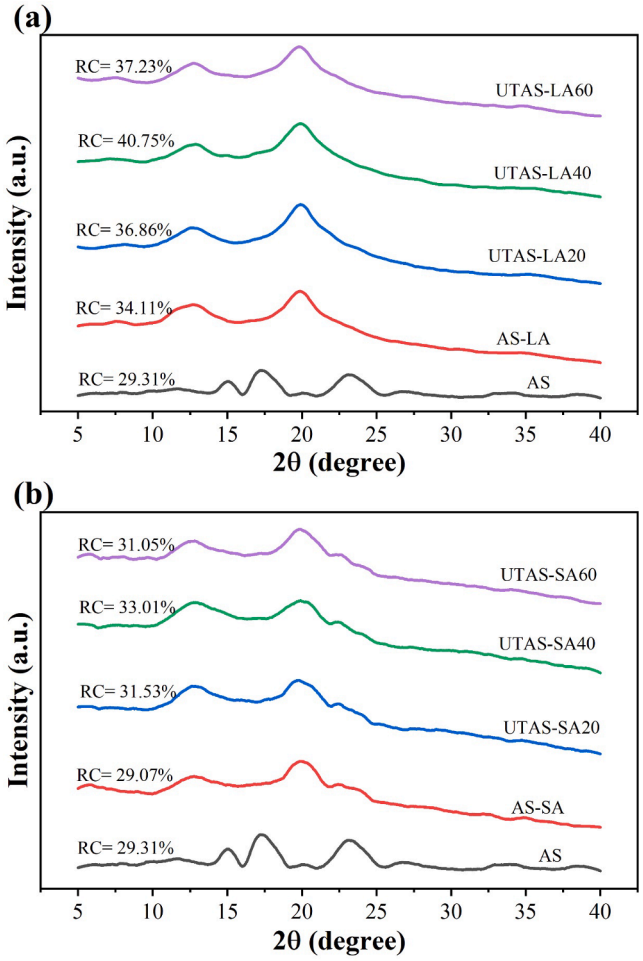

Fig. 3. XRD patterns and degree of relative crystallinity (RC) of (a) AS-LA complexes (b) AS-SA complexes.

compared to the lipid in the solid phase. The RC values ranged from 34.11% to 40.75% for LA-complexes and 29.07% to 33.01% for SA-complexes, while the RC value of AS was 29.31%. The highest RC value was found in UTAS-LA40, indicating better complexibility of liquid lipid at sonication time of 40 min. The results were further affirmed by the particle size distribution (Table 3), where the diameter at D(50) was significantly larger in UTAS-LA40 than the rest of the samples resulting in the stronger formation of LA with starch granules as clumps or aggregation. Another reason for liquid lipids to form better complexes is their smaller size compared to solid lipids, which helped them easily entrap in the hydrophobic cavities of the starch [21]. The RC of AS-SA-complexes was increased with corresponding rises in sonication times from 20 to 60 min. The ultrasonication increased leaching out of the amylose content to interact with lipids while degrading the amylopectin. However, in the case of UTAS-LA60, the formation of the bubble by sonication was so big that the time available for its collapse was insufficient to break the gelatin cluster [22]. Furthermore, the sonicated complexes showed a better degree of structural order resulting in stronger interactions between AS and fatty acids that are likely to reduce the susceptibility of complex to enzymatic digestion. Hence it was implied based on *in vitro* digestibility results that as compared to the reference (AS), all sonicated samples showed increasing tendencies in RS contents whereas exhibited decreasing trends in RDS contents. This indicated that UTAS-LA and UTAS-SA V-type complexes were found to exhibit a possibly higher degree of resistance to digestion as compared to AS and LA due to partial RDS convention to RS.

3.3. FTIR spectra of AS and starch-lipid complexes to understand the changes in short-range ordered structure

The spectra of AS with LA and SA complexes are shown in Fig. 4 (a, b), and their specific bands at different wavenumbers in Table 2. Two additional peaks were found for starch-lipid complexes; peak one at 2856–2851 cm^{-1} and 2850 cm^{-1}, and peak two at 1716 cm^{-1} for starch complexes with LA and SA, respectively. One broader peak at 3354 cm^{-1} for AS was associated with hydroxyl groups, while the peak at 3420 cm^{-1} appeared as a result of stretching vibrations of the O–H groups in starch-lipid complexes. The bands at 2850 cm^{-1} and 1716 cm^{-1} were linked to stretching vibrations of C–H and C = O of lipids as discussed previously [29,30]. The intensities of the bands decreased for all complexes as compared with AS. The absorbance was further reduced with increasing sonication time, and it was more obvious for LA complexes. This could be due to the increase in hydrophobicity of lipids as a result of UT, which is consistent with the results of XRD and CI. Furthermore, the decrease in absorbance in LA-complexes is more prominent, suggesting the ability of liquid fatty acids to form better complexes. The weaker band intensities further clarified the stronger interaction of unsaturated lipids and arrowhead starch in a crystalline network that could ultimately reduce the accessibility of the enzymes, hence slowing down the digestibility.

Furthermore, the short-range ordered structure of AS and starch-fatty acid complexes were analyzed by employing a deconvoluted spectrum in the spectral regions of 1200–800 cm^{-1}. The IR absorbance ratios at 1045/1022 cm^{-1} and 1022/995 cm^{-1} were shown in Table 1. The presence of the crystalline and amorphous regions in the starch molecules was corresponded by the IR spectral regions of 1045 cm^{-1} and 1022 cm^{-1}, respectively. An increase in the IR ratios of 1045/1022 cm^{-1} was found for all complexes with the profound increase in LA-complexes, whereas the ratios of 1022/995 cm^{-1} decreased for all complexes relative to AS, showing an increased degree of short-range molecular order, which was endorsed by the XRD results.

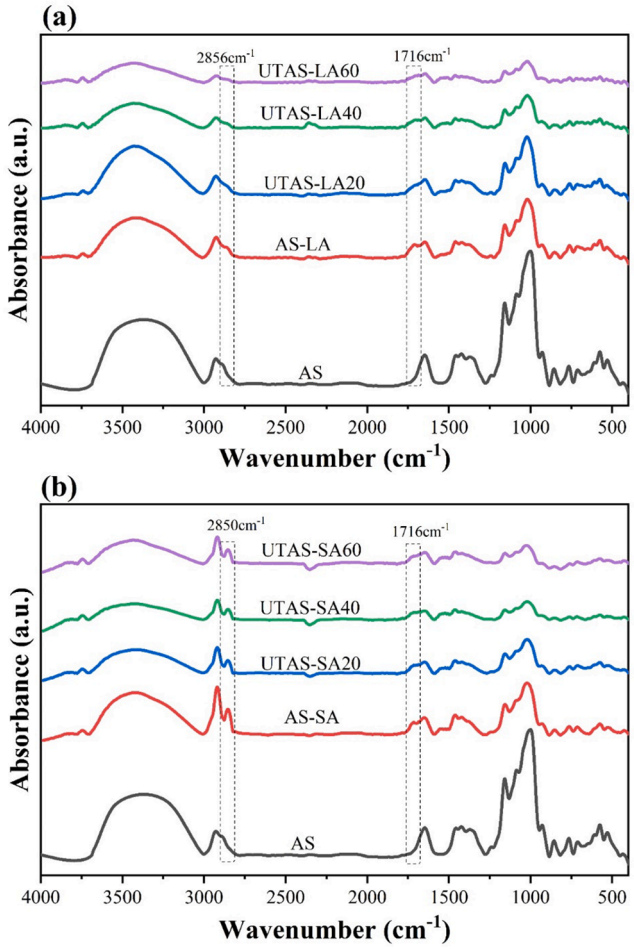

Fig. 4. FTIR spectra of arrowhead starch and starch-linoleic/stearic acid complexes.

Table 1
Changes in color and IR ratios.

Sample	L^*	a^*	b^*	IR ratio 1022/995 cm^{-1}	IR ratio 1045/1022 cm^{-1}
AS	96.47 ± 0.07a	−0.14 ± 0.00c	3.87 ± 0.03 g	1.750 ± 0.007a	0.767 ± 0.009c
AS-LA	94.72 ± 0.46bc	−0.23 ± 0.02d	7.18 ± 0.03b	1.293 ± 0.006c	0.808 ± 0.006ab
UTAS-LA20	94.67 ± 0.39bc	−0.45 ± 0.04f	7.10 ± 0.09b	1.268 ± 0.002de	0.796 ± 0.005b
UTAS-LA40	94.40 ± 0.02 cd	−0.39 ± 0.00e	6.63 ± 0.01d	1.248 ± 0.002f	0.814 ± 0.004a
UTAS-LA60	93.56 ± 0.56e	−0.40 ± 0.01e	7.74 ± 0.23a	1.265 ± 0.004e	0.814 ± 0.007a
AS-SA	95.16 ± 0.26b	0.05 ± 0.02a	4.33 ± 0.16f	1.310 ± 0.003b	0.775 ± 0.006c
UTAS-SA20	94.93 ± 0.35bc	−0.03 ± 0.01b	4.62 ± 0.13e	1.295 ± 0.005c	0.778 ± 0.006c
UTAS-SA40	94.69 ± 0.01bc	−0.03 ± 0.01b	4.87 ± 0.04d	1.256 ± 0.004e	0.797 ± 0.008b
UTAS-SA60	93.94 ± 0.08de	−0.21 ± 0.01d	4.47 ± 0.00ef	1.275 ± 0.003d	0.775 ± 0.006c

AS, arrowhead starch; AS-LA, arrowhead starch-linoleic acid complex; UTAS-LA20, arrowhead starch-linoleic acid complex UT for 20 min; UTAS-LA40, arrowhead starch-linoleic acid complex UT for 40 min; UTAS-LA60, arrowhead starch-linoleic acid complex UT for 60 min; AS-SA, arrowhead starch-stearic acid complex; UTAS-SA20, arrowhead starch-stearic acid complex UT for 20 min; UTAS-SA40, arrowhead starch-stearic acid complex UT for 40 min; UTAS-SA60, arrowhead starch-stearic acid complex UT for 60 min.

3.4. Psds of the starch-lipid complex at different ultrasonication times

The PSD of AS and AS-complexes with LA and SA are shown in Fig. 5. The results of the particle size distribution of D[3,2], D[4,3], and D(50) are given in Table 3. Compared to AS, an increase in the granule size was observed for all starch composites. The D(50) of LA-complexes decreased from 24.25 μm to 19.05 μm, whereas the D(50) of SA-complexes reduced from 19.90 μm to 18.20 μm after the increase in ultrasonication time from 40 min to 60 min. The median diameters D (50) of AS-LA and AS-SA were 22.35 μm and 16.50 μm, respectively. It could be seen from the results that the granule size of LA-complexes was much bigger than SA-complexes, probably due to agglomeration or clumping of starch and lipid particles, which could be further seen by the results of SEM. Our present results of *in-vitro* starch digestibility indicated that the increase in the granule size might be may lead to a reduction in contact between the enzymes and substrate as well as influence of particle size increase on digestibility where the complexes showed resistance against the enzymatic digestion, ultimately increasing the RS contents compared with native starch. The effect of particle size on the digestibility of starch was also discussed by Ma et al. [31] who concluded that a rising tendency in the size of granules could reduce the contact between the substrate and the enzymes. Our present results of *in-vitro* starch digestibility indicated the same effect of the increase in particle size on digestibility where the complexes showed resistance against the enzymatic digestion, ultimately increasing the RS contents compared with native starch [32].

3.5. Microstructure morphology

The morphological changes in the arrowhead starch and its complexes with lipids could be seen in Fig. 6a-i. The images are shown at a

Table 2
Changes in the functional groups.

Functional group	AS	AS-LA	UTAS-LA20	UTAS-LA40	UTAS-LA60	AS-SA	UTAS-SA20	UTAS-SA40	UTAS-SA60
OH	3354	3420	3420	3420	3420	3420	3420	3420	3420
C–H	2929	2927	2926	2924	2920	2917	2917	2917	2917
CH	——	2856	2856	2855	2851	2850	2850	2850	2850
C = O ketone	——	1716	1716	1716	1716	1716	1716	1716	1716
C = O amide	1647	1646	1647	1646	1647	1647	1647	1647	1646
CH3 bend	1362	1457	1457	1457	1457	1457	1457	1457	1457
C-O	1158	1157	1158	1158	1158	1158	1157	1159	1158
C-O–H	1081	1082	1081	1082	1082	1081	1081	1083	1082
OH	1015	1022	1020	1020	1020	1022	1021	1019	1020
C = C bending	930	933	934	938	939	935	936	939	938
C–C	861	863	863	865	867	863	864	866	865
C-O	763	760	760	760	760	759	759	759	759
C-O-C	575	575	575	575	575	575	575	575	575

AS, arrowhead starch; AS-LA, arrowhead starch-linoleic acid complex; UTAS-LA20, arrowhead starch-linoleic acid complex UT for 20 min; UTAS-LA40, arrowhead starch-linoleic acid complex UT for 40 min; UTAS-LA60, arrowhead starch-linoleic acid complex UT for 60 min; AS-SA, arrowhead starch-stearic acid complex; UTAS-SA20, arrowhead starch-stearic acid complex UT for 20 min; UTAS-SA40, arrowhead starch-stearic acid complex UT for 40 min; UTAS-SA60, arrowhead starch-stearic acid complex UT for 60 min.

Table 3
The particle size distribution of starch-lipid complex at different ultrasonication times.

Sample	D [3,2]	D [4,3]	D(10)	D(50)	D(90)
AS	6.36 ± 0.08d	11.70 ± 0.14d	3.665 ± 0.16e	10.25 ± 0.21d	21.60 ± 0.28d
AS-LA	13.60 ± 0.14ab	40.45 ± 4.74bc	5.71 ± 0.04bc	22.35 ± 0.35ab	94.75 ± 5.59b
UTAS-LA40	14.45 ± 1.48a	46.30 ± 26.16ab	5.96 ± 0.38ab	24.15 ± 3.18a	100.65 ± 21.71b
UTAS-LA60	13.85 ± 0.07a	68.50 ± 7.78a	6.12 ± 0.01a	19.05 ± 2.47bc	161.00 ± 11.31a
AS-SA	10.90 ± 0.71c	15.90 ± 4.24 cd	4.94 ± 0.20d	16.50 ± 1.13c	47.90 ± 13.86c
UTAS-SA40	12.25 ± 0.07bc	26.30 ± 0.14bcd	5.36 ± 0.03c	19.90 ± 0.14bc	53.40 ± 0.85c
UTAS-SA60	11.75 ± 0.07c	22.80 ± 0.71bcd	5.40 ± 0.02c	18.20 ± 0.00c	45.80 ± 0.85 cd

AS, arrowhead starch; AS-LA, arrowhead starch-linoleic acid complex; UTAS-LA40, arrowhead starch-linoleic acid complex UT for 40 min; UTAS-LA60, arrowhead starch-linoleic acid complex UT for 60 min; AS-SA, arrowhead starch-stearic acid complex; UTAS-SA40, arrowhead starch-stearic acid complex UT for 40 min; UTAS-SA60, arrowhead starch-stearic acid complex UT for 60 min.

resolution of 100 μm and 10 μm diameter for all samples. The AS exhibited round or oval shapes Fig. 6a, and their particle size ranged from 3.5 μm to 21.5 μm with an average size of 10 μm. On the other hand, the SEM micrographs of LA-complex were presented in Fig. 6b-e and SA-complex in Fig. 6f-i. There was a significant increase in the sizes of the granules for the complexes, as discussed in the previous section. The complexes further showed the phenomenon of reorientation and crystallization. Although the granules of both the LA and SA complexes were aggregated into bigger particles but LA showed a better crystalline arrangement compared with SA. The presence of free fatty acid aggregates could be seen in micrographs of stearic acid complexes. Furthermore, the LA-complexes had a sponge-like structure with smooth surfaces, while the SA-complexes exhibited flaky structures with irregular shapes and rough surfaces. Zhao et al. [22], while studying the effect of ultrasound-microwave treatment on starch-green tea polyphenol, also reported the increase in particle size and agglomeration of spherical crystalline particles. Chen et al. [26] also observed the aggregated spherulites formation of lotus starch-fatty acid complexes as a result of microfluidization.

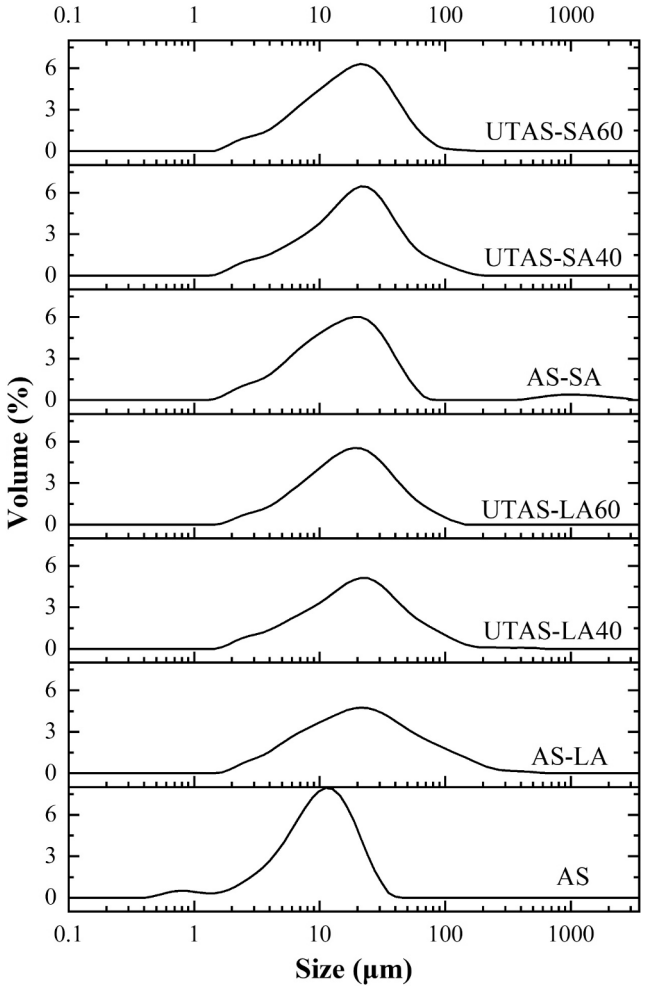

Fig. 5. Particle size distributions of native starch and its complexes with linoleic/stearic acid.

3.6. Thermograms of sonicated complexes

The parameters of thermal transitions for AS and its complexes with LA and SA are presented in Table 4. AS showed the single endothermic peak centered at 67.35 °C. Compared to AS, the complexes showed higher temperatures, suggesting that LA and SA could produce a more

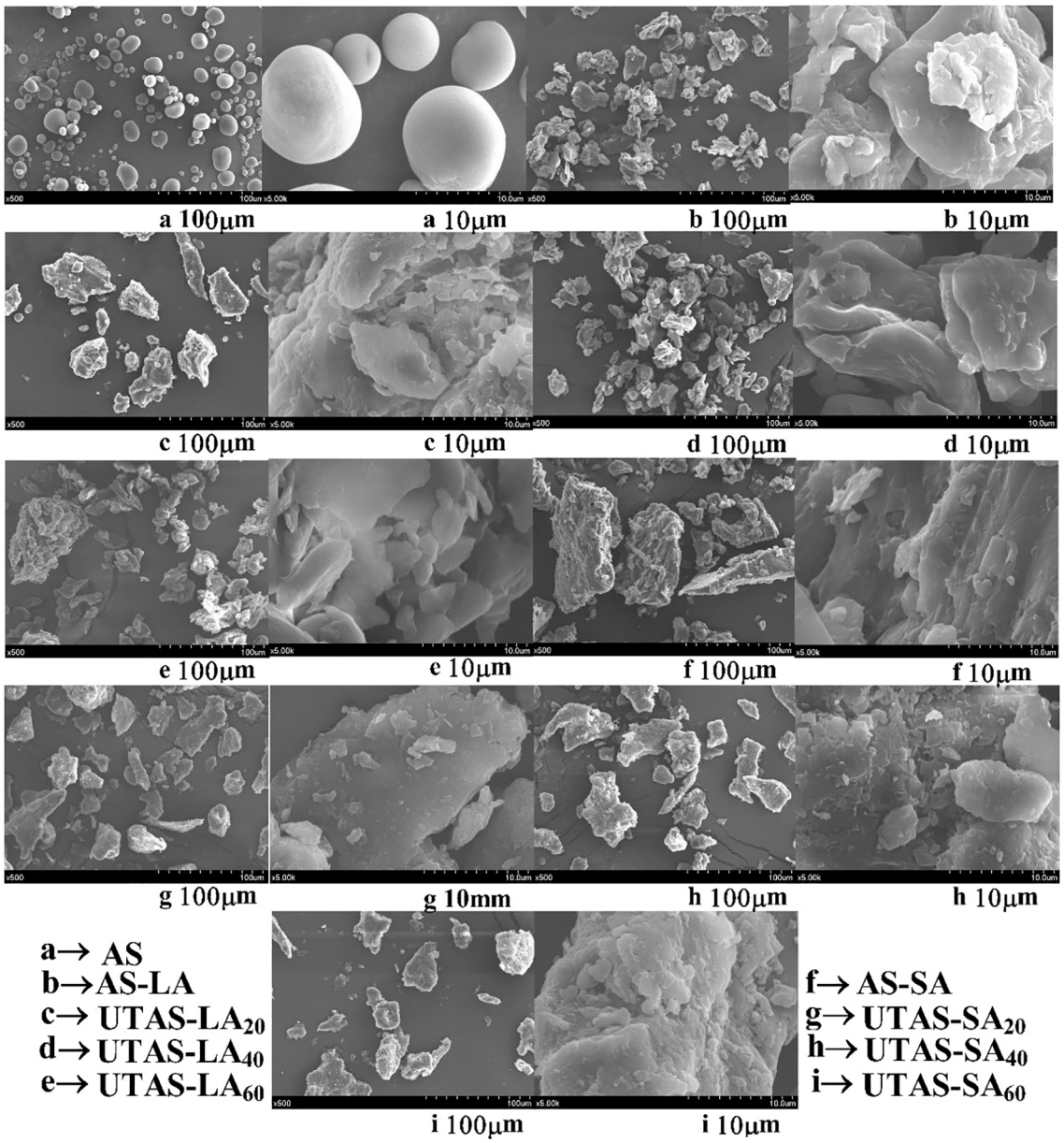

Fig. 6. Effects of DFPU SEM micrographs of native arrowhead starch and starch-linoleic/stearic acid complexes.

ordered and compact structure. Previous studies have shown the formation of V6-type I and II complexes when fatty acids are incorporated with starch [33]. In our study, the formation of V6 type (V6-I, II) complexes was observed. UTAS-LA showed the formation of type II V6-complex with (T_o = 103.83 °C to 112.77 °C), (T_p = 113.79 °C to 116.51 °C) and ($T_{c=}$ 118.64 °C to 129.12 °C). Furthermore, peak temperatures (Tp) values for type I V6-complexes for LA-complexes and SA-complexes were 80.77 °C to 85.47 °C and 83.47 °C 84.31 °C, respectively. An increase in T_p for both LA and SA complexes exhibited the effect of sonoprocessing. The effect was most obvious for LA-complexes which means the UT was more suitable for altering the properties of complexes formed with liquid lipids. The increase in T_p could further be associated with increased interactions of amylose with the lipids and a reduction in mobility of amylopectin chains [34].

The values of ΔT were higher for the complexes of LA compared to SA. The melting enthalpies ΔH were decreased for the complexes compared to AS, but an increasing trend could be seen with the increase in sonication time from 20 to 60 min except for UTAS-LA60 where ΔH was 1.333 J/g for peak 1 and 0.197 J/g for peak 2. The rise in ΔH values with increasing reaction time was also observed by [35] while studying the effect of enzymatic debranching on starch-stearic acid complex formation. The formation of type II complexes in starch-linoleic acids was noticed as an aggregate of type I complexes and was more ordered in structure, which could be further seen by the results of XRD where the peak intensities at 2θ° were significantly higher.

3.7. Changes in color

The changes in color parameters as a result of lipids inclusion in arrowhead starch at different sonication times are presented in Table 1. The colors were identified according to CIELAB color space index where the values of L^* accounted for lightness (black to white, 0–100), a^* (green to red, $-a^*$ to $+a^*$), and b^* (blue to yellow, $-b^*$ to $+b^*$). The values of L^* decreased for all complexes compared to AS. Although the decrease in L^* was non-significant among complexes, UTAS-LA60 exhibited the lowest value, 93.56. The reduction in lightness could be associated with the formation of the complexes. Furthermore, a significant increase in yellowness ($+b^*$) for complexes was observed. The

Table 4
Thermal properties of AS and AS-linoleic/stearic acid complexes under dual-frequency power ultrasound.

	Peak 1				Peak 2				ΔH total
Sample	*To*	*Tp*	*Tc*	*ΔH*	*To*	*Tp*	*Tc*	*ΔH*	
AS	53.35 ± 0.318f	67.35 ± 0.537f	82.52 ± 0.268f	4.259 ± 0.011a	ND	ND	ND	ND	4.259
AS-LA	72.27 ± 0.240e	80.77 ± 0.311e	89.86 ± 0.127c	1.135 ± 0.006 h	103.83 ± 0.417c	113.19 ± 0.490b	129.12 ± 0.593a	0.338 ± 0.008a	1.473
UTAS-LA20	73.03 ± 0.249e	82.345 ± 0.318d	91.10 ± 0.311b	1.221 ± 0.013 g	105.83 ± 0.474b	115.17 ± 0.368ab	125.30 ± 0.368b	0.317 ± 0.006a	1.538
UTAS-LA40	76.49 ± 0.156d	85.06 ± 0.382ab	93.61 ± 0.396a	1.442 ± 0.014e	112.59 ± 0.191a	116.51 ± 0.382a	119.39 ± 0.516c	0.219 ± 0.006b	1.661
UTAS-LA60	78.77 ± 0.177b	85.47 ± 0.042a	94.130.092a	1.333 ± 0.008f	112.77 ± 0.191a	115.72 ± 0.247a	118.64 ± 0.544c	0.197 ± 0.008c	1.530
AS-SA	79.51 ± 0.177ab	83.47 ± 0.184 cd	88.00 ± 0.049e	1.575 ± 0.005d	ND	ND	ND	ND	1.575
UTAS-SA20	79.75 ± 0.311a	83.87 ± 0.156c	88.54 ± 0.106de	1.621 ± 0.006c	ND	ND	ND	ND	1.621
UTAS-SA40	79.25 ± 0.134ab	84.08 ± 0.134bc	89.36 ± 0.290 cd	1.651 ± 0.003c	ND	ND	ND	ND	1.651
UTAS-SA60	77.47 ± 0.141c	84.31 ± 0.141bc	91.16 ± 0.240b	1.737 ± 0.008b	ND	ND	ND	ND	1.737

AS, arrowhead starch; AS-LA, arrowhead starch-linoleic acid complex; UTAS-LA20, arrowhead starch-linoleic acid complex UT for 20 min; UTAS-LA40, arrowhead starch-linoleic acid complex UT for 40 min; UTAS-LA60, arrowhead starch-linoleic acid complex UT for 60 min; AS-SA, arrowhead starch-stearic acid complex; UTAS-SA20, arrowhead starch-stearic acid complex UT for 20 min; UTAS-SA40, arrowhead starch-stearic acid complex UT for 40 min; UTAS-SA60, arrowhead starch-stearic acid complex UT for 60 min.

values of b^* ranged from 6.63 to 7.74 and 4.33–4.87 for LA and SA complexes, respectively. It could be seen that the increase in yellowness was more prominent for linoleic acid complexes, and the highest value of $+ b^*$ was found in UTAS-LA60. The rising trend in degrees of yellowness and redness while a decrease in the degree of lightness might be ascribed to the probable presence of pigments that leached into the starch-lipid complexes after exposure to vibration amplitude of power ultrasound. Sonication caused enhanced leaching because of increased cavitation which exerted significant influence on rupturing of the surfaces of the starch granules which led to mass transfer of solutes including pigment compounds through granular cracks existing in starch granules and hence coloration of starch-lipid complexes was significantly affected [17]. Moreover, the coloration changes after exposure of power ultrasound to starch granules have been reported by the previously published report [36].

3.8. AS-LA and AS-SA complexes in-vitro digestibility

The glycaemic response is usually influenced by starch fractions (RS, SDS, and RDS). Digestibility or rate of digestion has been regarded as one of the most influential determinants of glycaemic response as this rate of digestion indicates the release rate and absorption of glucose and maltose in the gut [7]. In vitro digestibility of arrowhead starch fractions (RS, SDS, and RDS) of AS, AS-LA, AS-SA, and UTAS samples is shown in Fig. 7. Compared to the reference (AS), all sonicated samples showed increasing tendencies in RS contents whereas exhibited decreasing

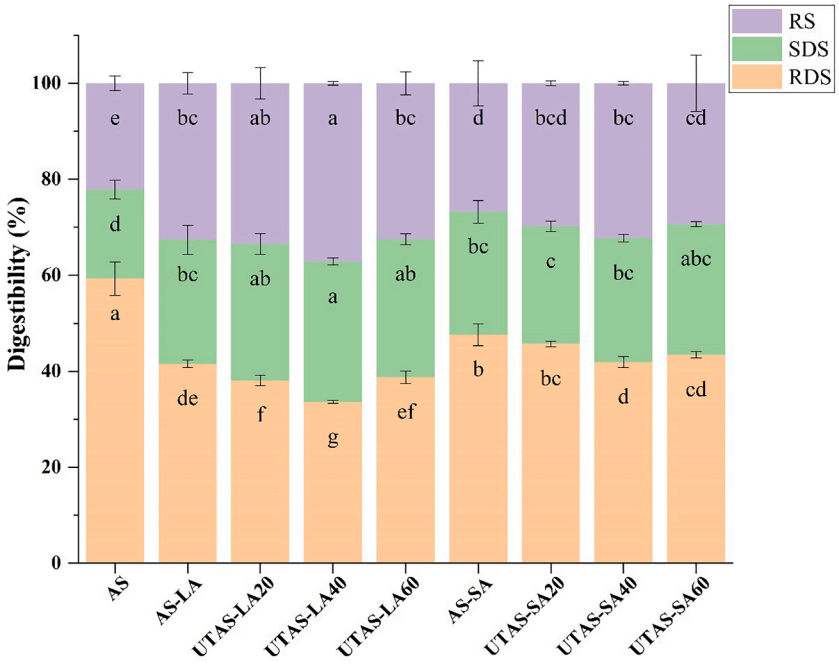

Fig. 7. Changes of *in-vitro* starch digestibility of AS and AS-LA/SA complexes.

trends in RDS contents. In comparison with the AS and LA, this indicated that the V-type complexes exhibited increased resistance to digestion possibly because of partial RDS convention to RS. These results are in agreement with the previously reported findings [7,29,32,34], which also demonstrated that starch-lipid complexes exhibited reduced digestion degree as compared to those of reference starch samples. In comparison with untreated AS-LA and AS-SA complexes, V-type complexes sonicated at 20/40 kHz for 40 min exhibited increasing proportions of RS with the highest content (37.14%) for UTAS-LA40.

Similarly, SDS contents of UTAS-LA and UTAS-SA samples showed a significantly ($p < 0.05$) rising tendency with corresponding increases in sonication time from 20 to 40 min as compared to the reference (AS) and untreated complexes (AS-LA and AS-SA). However, the SDS contents after sonication were higher in linoleic acid complexes compared to stearic acid and UTAS-LA40 exhibited the highest proportions of SDS (29.25%). Moreover, the decreases in RDS were more prominent for the LA complexes than SA, providing evidence of a more crystalline structure formed by liquid fatty acids to inhibit enzymatic activity. Conclusively, it may be implied from these results that variations in applied sonication time and fatty acid structures significantly influenced the degree of digestibility of inclusion complexes.

4. Conclusions

Ultrasound can change the starch's physicochemical properties, ultimately changing the supramolecular structure and making the starch susceptible to enzymatic hydrolysis depending on the treatment conditions of ultrasound. Dual-frequency (DFPU) at 20/40 kHz for different treatment times of 20, 40, and 60 min was used to systematically understand the sonication effects on the multi-scale structure of the composites and the influence of these interactions on physicochemical, structural, and *in-vitro* digestibility of the starch-lipid complexes prepared with arrowhead starch, linoleic and stearic acids. The XRD results revealed the V-type crystalline structure with prominent peaks at $2\theta = 13.0^{\circ}$ and 20.0° and short-range ordered structure was observed as an increase in IR ratios of 1045/1022 cm^{-1} by FTIR spectroscopy. The complexing index values were increased when the samples were treated with DFPU, and the UTAS-LA40 showed a better CI value. SEM results revealed a flaky structure with irregular shapes and rough surfaces. Significant rises in RS contents were discovered as a result of DFPU. The current study results could possibly be employed for developing new RS-incorporated products through an eco-friendly non-thermal method.

CRediT authorship contribution statement

Husnain Raza: Investigation, Methodology, Writing – original draft, Writing – review & editing. **Qiufang Liang:** Investigation, Writing – original draft, Writing – review & editing, Data curation. **Kashif Ameer:** Writing – review & editing. **Haile Ma:** Supervision, Writing – review & editing. **Xiaofeng Ren:** Conceptualization, Funding acquisition, Project administration, Resources, Supervision.

Declaration of Competing Interest

The authors declare that they have no known competing financial interests or personal relationships that could have appeared to influence the work reported in this paper.

Acknowledgment

The authors wish to express their appreciation for the support obtained from the National Natural Science Foundation of China (Grants No. 32072355&31771977); The Jiangsu agricultural science and technology innovation fund (Grants No. CX (20) 3044); The Primary Research & Development Plan of Zhenjiang (Grants No. NY2020011); Sponsored by Key Laboratory of Modern Agricultural Equipment and Technology (Jiangsu University); Sponsored by Qing Lan Project (2020); Jiangsu Province Postdoctoral Science Foundation Special Funding Project (2019K114); Priority Academic Program Development of Jiangsu Higher Education Institutions (PAPD). There are no conflicts of interest to declare. This article does not contain any studies involving human or animal subjects.

References

[1] C.D. Cook, Aquatic plant book, SPB Academic Pub., 1996.
[2] J. Gu, H. Zhang, J. Zhang, C. Wen, H. Ma, Y. Duan, Y. He, Preparation, characterization and bioactivity of polysaccharide fractions from Sagittaria sagittifolia L, Carbohydr. Polym. 229 (2020), 115355.
[3] I.A. Wani, A.A. Wani, A. Gani, S. Muzzaffar, M.K. Gul, F.A. Masoodi, T.A. Wani, Effect of gamma-irradiation on physico-chemical and functional properties of arrowhead (Sagittaria sagittifolia L.) tuber flour, Food bioscience 11 (2015) 23–32.
[4] I.A. Wani, A. Gani, A. Tariq, P. Sharma, F.A. Masoodi, H.M. Wani, Effect of roasting on physicochemical, functional and antioxidant properties of arrowhead (Sagittaria sagittifolia L.) flour, Food Chem. 197 (2016) 345–352.
[5] J. Zhang, M. Chen, C. Wen, J. Zhou, J. Gu, Y. Duan, H. Zhang, X. Ren, H. Ma, Structural characterization and immunostimulatory activity of a novel polysaccharide isolated with subcritical water from Sagittaria sagittifolia L, Int. J. Biol. Macromol. 133 (2019) 11–20.
[6] C. Wen, J. Zhang, J. Zhou, M. Cai, Y. Duan, H. Zhang, H. Ma, Antioxidant activity of arrowhead protein hydrolysates produced by a novel multi-frequency S-type ultrasound-assisted enzymolysis, Nat. Prod. Res. 34 (20) (2020) 3000–3003.
[7] Y. Ding, Y. Liang, F. Luo, Q. Ouyang, Q. Lin, Understanding the mechanism of ultrasonication regulated the digestibility properties of retrograded starch following vacuum freeze drying, Carbohydr. Polym. 228 (2020), 115350.
[8] H.N. Englyst, S. Kingman, J. Cummings, Classification and measurement of nutritionally important starch fractions, Eur. J. Clin. Nutr. 46 (1992) S33–50.
[9] X. Chen, X. He, X. Fu, B. Zhang, Q. Huang, Complexation of rice starch/flour and maize oil through heat moisture treatment: Structural, in vitro digestion and physicochemical properties, Int. J. Biol. Macromol. 98 (2017) 557–564.
[10] N. López-Barón, Y. Gu, T. Vasanthan, R. Hoover, Plant proteins mitigate in vitro wheat starch digestibility, Food Hydrocolloids 69 (2017) 19–27.
[11] B. Zheng, T. Wang, H. Wang, L. Chen, Z. Zhou, Studies on nutritional intervention of rice starch- oleic acid complex (resistant starch type V) in rats fed by high-fat diet, Carbohydr. Polym. 246 (2020), 116637.
[12] N. Noor, A. Gani, F. Jhan, J.L.H. Jenno, M. Arif Dar, Resistant starch type 2 from lotus stem: Ultrasonic effect on physical and nutraceutical properties, Ultrasonics Sonochemistry, 76 (2021) 105655.
[13] S.R. Falsafi, Y. Maghsoudlou, H. Rostamabadi, M.M. Rostamabadi, H. Hamedi, S.M. H. Hosseini, Preparation of physically modified oat starch with different sonication treatments, Food Hydrocolloids 89 (2019) 311–320.
[14] F. Zhu, Impact of ultrasound on structure, physicochemical properties, modifications, and applications of starch, Trends Food Sci. Technol. 43 (2015) 1–17.
[15] W. Zhu, X. Xue, Z. Zhang, Ultrasonic-assisted extraction, structure and antitumor activity of polysaccharide from Polygonum multiflorum, Int. J. Biol. Macromol. 91 (2016) 132–142.
[16] P. Liu, R. Wang, X. Kang, B. Cui, B. Yu, Effects of ultrasonic treatment on amylose-lipid complex formation and properties of sweet potato starch-based films, Ultrason. Sonochem. 44 (2018) 215–222.
[17] H. Raza, K. Ameer, H. Ma, Q. Liang, X. Ren, Structural and Physicochemical Characterization of Modified Starch from Arrowhead Tuber (Sagittaria sagittifolia L.) using Tri-Frequency Power Ultrasound, Ultrason. Sonochem. 80 (2021).
[18] A.P. Bonto, R.N. Tiozon, N. Sreenivasulu, D.H. Camacho, Impact of ultrasonic treatment on rice starch and grain functional properties: A review, Ultrason. Sonochem. 71 (2021).
[19] H. Wang, Y. Liu, L. Chen, X. Li, J. Wang, F. Xie, Insights into the multi-scale structure and digestibility of heat-moisture treated rice starch, Food Chem. 242 (2018) 323–329.
[20] R. Wang, P. Liu, B. Cui, X. Kang, B. Yu, Effects of different treatment methods on properties of potato starch-lauric acid complex and potato starch-based films, Int. J. Biol. Macromol. 124 (2019) 34–40.
[21] X. Kang, P. Liu, W. Gao, Z. Wu, B. Yu, R. Wang, B. Cui, L. Qiu, C. Sun, Preparation of starch-lipid complex by ultrasonication and its film forming capacity, Food Hydrocolloids 99 (2020), 105340.
[22] B. Zhao, S. Sun, H. Lin, L. Chen, S. Qin, W. Wu, B. Zheng, Z. Guo, Physicochemical properties and digestion of the lotus seed starch-green tea polyphenol complex under ultrasound-microwave synergistic interaction, Ultrason. Sonochem. 52 (2019) 50–61.
[23] X. Kong, Starches Modified by Nonconventional Techniques and Food Applications, in: Starches for Food Application, Elsevier, 2019, pp. 271-295.
[24] W. Qin, C. Wen, J. Zhang, C.S. Dzah, H. Zhang, Y. He, Y. Duan, Structural characterization and physicochemical properties of arrowhead resistant starch prepared by different methods, Int. J. Biol. Macromol. 157 (2020) 96–105.
[25] H.N. Englyst, J.H. Cummings, Digestion of the polysaccharides of some cereal foods in the human small intestine, The American journal of clinical nutrition 42 (1985) 778–787.

[26] B. Chen, Z. Guo, S. Miao, S. Zeng, X. Jia, Y. Zhang, B. Zheng, Preparation and characterization of lotus seed starch-fatty acid complexes formed by microfluidization, J. Food Eng. 237 (2018) 52–59.
[27] S. Sun, Y. Jin, Y. Hong, Z. Gu, L. Cheng, Z. Li, C. Li, Effects of fatty acids with various chain lengths and degrees of unsaturation on the structure, physicochemical properties and digestibility of maize starch-fatty acid complexes, Food Hydrocolloids 110 (2021), 106224.
[28] P. Liu, X. Kang, B. Cui, R. Wang, Z. Wu, Effects of glycerides with different molecular structures on the properties of maize starch and its film forming capacity, Ind. Crops Prod. 129 (2019) 512–517.
[29] M. Zheng, C. Chao, J. Yu, L. Copeland, S. Wang, S. Wang, Effects of chain length and degree of unsaturation of fatty acids on structure and in vitro digestibility of starch–protein–fatty acid complexes, J. Agric. Food. Chem. 66 (2018) 1872–1880.
[30] S. Sun, Y. Jin, Y. Hong, Z. Gu, L.i. Cheng, Z. Li, C. Li, Effects of fatty acids with various chain lengths and degrees of unsaturation on the structure, physicochemical properties and digestibility of maize starch-fatty acid complexes, Food Hydrocolloids 110 (2021) 106224.
[31] M. Ma, Y. Wang, M. Wang, J.-L. Jane, S.-K. Du, Physicochemical properties and in vitro digestibility of legume starches, Food Hydrocolloids 63 (2017) 249–255.
[32] H. Raza, K. Ameer, X. Ren, Q. Liang, X. Chen, H. Chen, H. Ma, Physicochemical properties and digestion mechanism of starch-linoleic acid complex induced by multi-frequency power ultrasound, Food Chem. 364 (2021), 130392.
[33] S. Wang, J. Wang, J. Yu, S. Wang, Effect of fatty acids on functional properties of normal wheat and waxy wheat starches: A structural basis, Food Chem. 190 (2016) 285–292.
[34] Y. Ai, J. Hasjim, J.-L. Jane, Effects of lipids on enzymatic hydrolysis and physical properties of starch, Carbohydr. Polym. 92 (2013) 120–127.
[35] C.K. Reddy, S.M. Choi, D.-J. Lee, S.-T. Lim, Complex formation between starch and stearic acid: Effect of enzymatic debranching for starch, Food Chem. 244 (2018) 136–142.
[36] A. Martins, C. Beninca, C.D. Bet, R.Z.B. Bisinella, C.S. de Oliveira, P.S. Hornung, E. Schnitzler, Ultrasonic modification of purple taro starch (Colocasia esculenta B. Tini): structural, physicochemical and thermal properties, J. Therm. Anal. Calorim. 142 (2020) 819–828.